

# **Activity of lipases and esterases towards tertiary alcohols: New insights into structure- function relationships\*\***

**Erik Henke, Jürgen Pleiss, Uwe T. Bornscheuer\***

[\*] Prof. Dr. U.T. Bornscheuer, Dr. E. Henke, Institute for  
Chemistry & Biochemistry, Dept. of Technical Chemistry &  
Biotechnology, Greifswald University, Soldmannstr. 16, D-17487  
Greifswald (Germany) Tel.: (+49) 3834-86-4367; Fax: (+49)  
3834-86-4346; E-mail: bornsche@uni-greifswald.de;

web: <http://www.chemie.uni-greifswald.de/~biotech>

Dr. J. Pleiss, Institute of Technical Biochemistry, Stuttgart  
University, Stuttgart (Germany)

*Dedicated to Prof. Rolf D. Schmid on the occasion of his 60<sup>th</sup>  
birthday*

[\*\*] We thank Prof. R. D. Schmid (Institute of Technical  
Biochemistry (ITB), Stuttgart University) for helpful  
discussions and Sandra Vorlová (ITB) for providing recombinant  
hAChE and bAChE. This work was financed by the German Research  
Foundation (DFG, Bonn, Germany, Grant Bo 1475/2-1).

Hydrolytic enzymes are versatile biocatalysts and find increasing applications in organic synthesis<sup>[1]</sup> and a considerable number of industrial processes using these enzymes have been commercialized.<sup>[2]</sup> Within this class, lipases (E.C. 3.1.1.3) and carboxyl esterases (E.C. 3.1.1.1) are frequently used as they accept a broad range of non-natural substrates, are usually very stable in organic solvents and exhibit good to excellent stereoselectivity. However, the vast majority of substrates are secondary alcohols followed by carboxylic acids and primary alcohols. Tertiary alcohols (TA) and their esters (TAEs) are a group of important compounds, which can be found in a number of natural products (e.g.,  $\alpha$ -terpineol, linalool) and occur in building blocks.<sup>[3]</sup> Unfortunately, only very few hydrolases have been shown to accept them as substrates.<sup>[4]</sup> Furthermore, reaction rates and/or enantioselectivities were quite low and consequently applications are rather unlikely. Structural reasons for the lack of activity and enantioselectivity of hydrolases towards these compounds have not been ruled out so far, despite the fact that the 3D-structures of several lipases and esterases are known since more than a decade.

Initially, we checked 25 commercially available enzyme preparations for their activity towards the four model acetates **1-4** (Scheme 1). In accordance with literature, we found that only a lipase from *Candida rugosa* (CRL)<sup>[4c, 4d]</sup> and lipase A from *Candida antarctica* (CAL-A)<sup>[4e]</sup> are active. The protein structure of CAL-A is unknown, sequence analysis shows

no major similarity to known proteins and it was shown by secondary structure analysis that this lipase lacks the common  $\alpha/\beta$ -hydrolase fold pattern.<sup>[5]</sup> Thus, further investigations were concentrated on the well-characterized CRL. Comparison of the 3D-structure of CRL with those enzymes not acting on esters of tertiary alcohols (TAEs) revealed that the alcohol binding pocket in CRL is 1.5 to 2 Å wider (Table 1), thus allowing the binding of the nearly spherical tertiary alcohol moiety. The amino acid sequence of CRL contains a GGGX-motif<sup>[6]</sup> that is positioned in the enzyme active center. This amino acid pattern, located on a protein loop near the binding site of the substrate ester's carboxylic group, is involved in the formation of the so-called oxyanion hole, which stabilizes the anionic carbonyl oxygen of the tetrahedral intermediate during the catalytic cycle of ester hydrolysis. The oxyanion and thus the whole intermediate is stabilized by two H-bonds which are provided by two amide groups of the protein backbone. In contrast, most commercial lipases and esterases have a GX-motif in this particular part of the active site.<sup>[6]</sup> Here a bulky residue (labeled X) forms the H-bond. So far, the GX- and GGGX-motifs and their occurrence in  $\alpha/\beta$ -hydrolases have been reported only in a phenomenological manner, but no direct linkage to catalytic properties of these enzymes have been identified.

Based on the structural differences of GGGX and GX-type  $\alpha/\beta$ -hydrolases a computer model was developed (see supplementary material for details). A thorough comparison of structural

data of CRL with inactive GX-hydrolases (e.g. lipase from *Pseudomonas cepacia* (PCL)) revealed that in GX-type hydrolases the backbone carbonyl oxygen of the X-residue (leucine in PCL) is orientated into the binding pocket at a location incorporating the C $_{\alpha}$  of the alcohol moiety of the substrate (Scheme 2a). In the case of a quarternary C $_{\alpha}$ , which is present in TAEs, a repulsive interaction between the carbonyl oxygen and the spherically arranged substituents of this C $_{\alpha}$  is observed. In CRL the GGGX-loop should provide a most flexible configuration, due to the short side-chain glycine residues, (Scheme 2b). Moreover the carbonyl oxygens are arranged parallel to the binding pocket, thus providing sufficient space at this critical part of the enzyme structure for the bulky tertiary alcohol group. This was verified first by computer simulation of substrate-enzyme complexes with GX- and GGGX-type esterases and lipases followed by experimental confirmation using a range of GGGX-type  $\alpha/\beta$ -hydrolases identified by amino acid sequence comparison using Internet-based public databases.

Thus discovered, acetylcholine esterases from three species (namely electric eel (*Electrophorus electricus*, eeAChE), banded krait (*Bungarus fasciatus*, bAChE) and human (hAChE)), carboxylesterases (*p*-nitrobenzylesterase from *B. subtilis* (BsubpNBE) and pig liver esterase (PLE)), and an additional lipase (from *Geotrichum candidum* (GCL)) were checked for activity in the hydrolysis of model acetates **1-4**. All PLE and eeAChE were used as commercial grade lyophilized powders, the

other enzymes were produced recombinantly in microbial expression systems. GCL<sup>[7]</sup>, bAChE and hAChE<sup>[8]</sup> were expressed in the methylotrophic yeast *Pichia pastoris*. The gene encoding BsubpNBE was cloned from genomic DNA from *B. subtilis* DSM 402 and expressed in high yields in *E. coli* (see supplementary material for details).

With the exception of GCL, all these GGGX-type  $\alpha/\beta$ -hydrolases hydrolyzed the model esters (Table 2). Only eeAChE showed no measurable activity towards *tert*-butyl acetate **1**, but this was also a poor substrate for the other biocatalysts. In contrast, substrates **2-4** were converted at high rates and up to 77% conversion were achieved (Table 3). The activity of BsubpNBE towards **4** was determined to be 3890 mU mg<sup>-1</sup> protein, the activity of the PLE preparation Chirazyme E-1 was 1640 mU mg<sup>-1</sup> protein, thus being 17 and 20 times more active towards **4** compared to *tert*-butyl acetate **1**.

An additional hint that the GGGX-motif is crucial for activity towards tertiary alcohols are the unsuccessful experiments to create activity by directed evolution<sup>[9]</sup> experiments based on GX-type esterases. For this, enzyme libraries of two genes encoding esterases from *Pseudomonas fluorescens*<sup>[10]</sup> and *Bacillus stearothermophilus*<sup>[11]</sup> were built using error-prone PCR<sup>[12]</sup> and DNA shuffling<sup>[13]</sup> methods and the proteins were then expressed using a strong rhamnose-inducible promoter.<sup>[14]</sup> However, no active mutants were identified after screening a library of approximately 15 000 esterase variants.

We have provided strong evidence, that the GGGX-motif described for some lipases does not only play a role in stabilizing the tetrahedral intermediate during catalysis, but also governs activity towards tertiary alcohols. With the exception of GCL-B, all tested esterases and lipases bearing the GGGX-motif hydrolyzed the model acetates.

Interestingly, GGGX-type hydrolases identified by this approach differ considerably in their overall substrate spectra. CRL is a typical lipase showing the lid mechanism and interfacial activation.<sup>[15]</sup> In contrast, PLE and BsubpNBE are typical carboxyl esterases showing highest activity towards medium and short-chain substrates with lower hydrophobicity, while AChEs are well known for their very narrow substrate range. This means in turn, that knowledge about their usual biocatalytic activity would not suggest that these enzymes would have activity towards tertiary alcohols in common.

Furthermore, they belong to different classes (carboxylesterases or lipases) and originate from mammals (acetylcholine esterase, pig liver esterase), bacteria (esterase from *Bacillus subtilis*) or yeast (lipases from *Candida rugosa* and *Geotrichum candidum*). The overall amino acid sequence similarity is rather low and only small regions around the GGGX-motif and the active serine are conserved.

The correlation between a simple amino acid pattern and activity towards tertiary alcohols is obviously interesting for researchers in the field of biocatalysis and organic synthesis. By simple comparison of amino acid sequences of

lipases and esterases, it is now possible to easily identify further enzymes, which are active towards tertiary alcohols.

Furthermore, we could already demonstrate, that our computer model also allows the prediction of mutants with enhanced or inversed stereoselectivity in the resolution of the model acetates of tertiary alcohols.<sup>[ 21]</sup>

## Experimental

All experimental details can be found in the supplementary material available from the Internet or the corresponding author.

## References

- [ 1] U. T. Bornscheuer, R. J. Kazlauskas, *Hydrolases in Organic Synthesis - Regio- and Stereoselective Biotransformations*, Wiley-VCH, Weinheim, **1999**.
- [ 2] A. Liese, K. Seelbach, C. Wandrey, *Industrial Biotransformations*, Wiley-VCH, Weinheim, **2000**.
- [ 3] A. J. Blacker, R. A. Holt, Zeneca ltd., Int. Patent Application WO 94/24305, **1994**.
- [ 4] a) M. Pogorevc, U. T. Strauss, M. Hayn, K. Faber, *Chem. Monthly* **2000**, *131*, 639-644; b) A. Schlacher, T. Stanzer, J. Osprian, M. Mischitz, E. Klingsbichel, K. Faber, H. Schwab, *J. Biotechnol.* **1998**, *62*, 47-54; c) D. O'Hagan, N. A. Zaidi, *Tetrahedron: Asymmetry* **1994**, *5*, 1111-1118; d) D. O'Hagan, N. A. Zaidi, *J. Chem. Soc. Perkin Trans. I*

- 1992**, 947-948; e) J. A. Bosley, J. Casey, A. R. Macrae, G. MyCock, US Patent Application US 5,658,769, **1997**.
- [ 5] D. L. Ollis, E. Cheah, M. Cygler, B. Dijkstra, F. Frolow, S. Franken, M. Harel, S. J. Remington, I. Silman, *Protein Eng.* **1992**, 5, 197-211.
- [ 6] J. Pleiss, M. Fischer, M. Peiker, C. Thiele, R. D. Schmid, *J. Mol. Catal. B: Enzym.* **2000**, 10, 491-508. The GGGX-motif sometimes contains an alanine (GGAX) instead of a glycine as exemplified in Table 1 for BsubpNBE.
- [ 7] E. Catoni, C. Schmidt-Dannert, S. Brocca, R. D. Schmid, *Biotechnol. Techn.* **1997**, 11, 689-695.
- [ 8] S. Vorlova, J. Schmitt, R. D. Schmid, submitted.
- [ 9] a) U. T. Bornscheuer, M. Pohl, *Curr. Opin. Chem. Biol.* **2001**, 5, 137-143; b) M. T. Reetz, *Angew. Chem.* **2001**, 113, 292-320; *Angew. Chem. Int. Ed. Engl.* **2001**, 40, 284-310; c) F. H. Arnold, A. A. Volkov, *Curr. Opin. Chem. Biol.* **1999**, 3, 54-59.
- [ 10] N. Krebsfänger, K. Schierholz, U. T. Bornscheuer, *J. Biotechnol.* **1998**, 60, 105-111.
- [ 11] Y. Amaki, E. E. Tulin, S. Ueda, K. Ohmiya, T. Yamane, *Biosci. Biotech. Biochem.* **1992**, 56, 238-241.
- [ 12] J.-P. Vartanian, M. Henry, S. Wain-Hobson, *Nucl. Acids Res.* **1996**, 24, 2627-2631.
- [ 13] a) W. P. C. Stemmer, *Nature* **1994**, 370, 389-391; b) H. Zhao, F. H. Arnold, *Nucl. Acids Res.* **1997**, 25, 1307-1308.
- [ 14] T. Stumpp, B. Wilms, J. Altenbuchner, *BioSpektrum* **2000**, 6, 33-36.



- [ 15] a) R. D. Schmid, R. Verger, *Angew. Chem.* **1998**, *110*, 1694-1720; *Angew. Chem. Int. Ed. Engl.* **1998**, *37*, 1608-1633; b) R. Verger, *Trends Biotechnol.* **1997**, *15*, 32-38.
- [ 16] P. Lebaron, J. F. Ghiglione, C. Fajon, N. Batailler, P. Normand, *FEMS Microbiol. Lett.* **1998**, *160*, 137-143.
- [ 17] J. Zock, C. Cantwell, J. Swartling, R. Hodges, T. Pohl, K. Sutton, P. Rosteck, Jr., D. McGilvray, S. Queener, *Gene* **1994**, *151*, 37-43.
- [ 18] U. T. Bornscheuer, J. Altenbuchner, H. H. Meyer, *Biotechnol. Bioeng.* **1998**, *58*, 554-559.
- [ 19] H.-C. Holzwarth, J. Pleiss, R.-D. Schmid, *J. Mol. Catal. B: Enzym.* **1997**, *3*, 73-82.
- [ 20] B. Spiller, A. Gershenson, F. H. Arnold, R. C. Stevens, *Proc. Natl. Acad. Sci. USA* **1999**, *96*, 12305-12310.
- [ 21] E. Henke, U. T. Bornscheuer, J. Pleiss, *Angew. Chem.* **2002**; *Angew. Chem. Int. Ed. Engl.* **2002**, submitted.

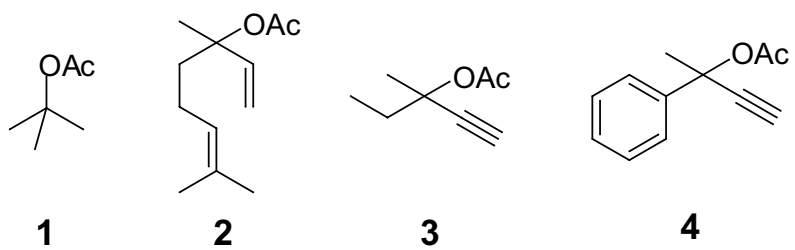
## LEGENDS FOR SCHEMES

**Scheme 1:** Esters of tertiary alcohols (TAEs) used as model substrates.

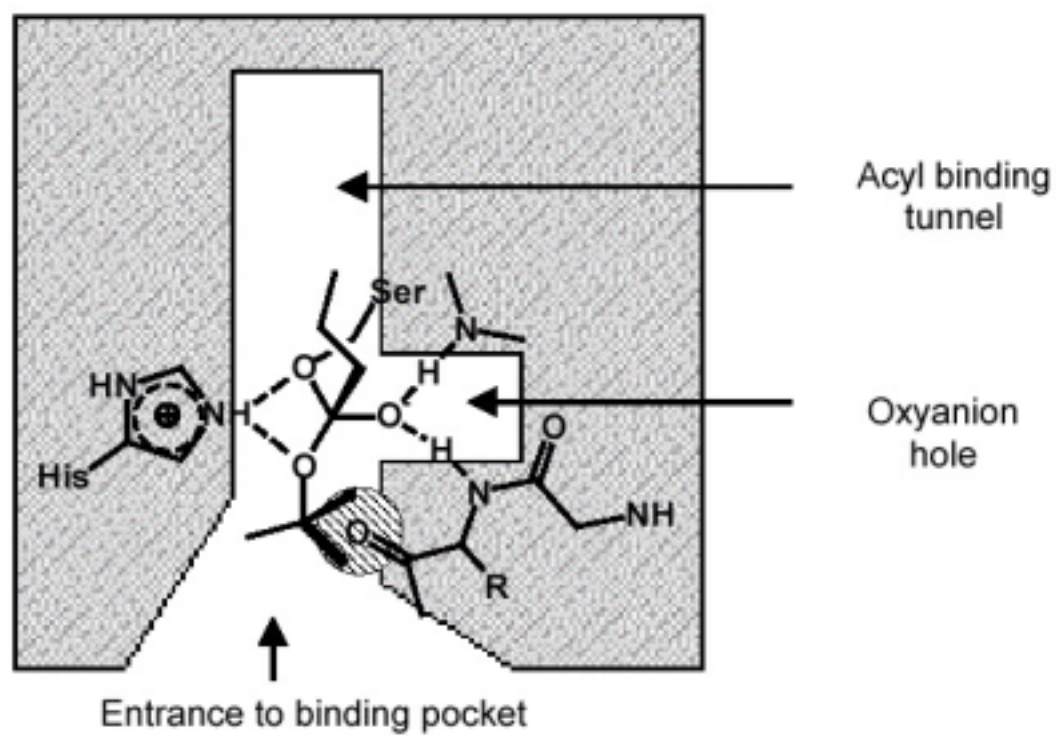
**Scheme 2a:** Schematic view into the binding pocket of GX-type hydrolases. The carbonyl oxygen of the oxyanion hole residue faces inwards the binding pocket of the alcohol moiety. Thus interaction of this oxygen with the quaternary C<sub>α</sub> of a TAE disables an appropriate binding of the substrate.

**Scheme 2b:** Schematic view into the binding pocket of GGGX type hydrolases (i.e CRL). The carbonyl backbone of the flexible triple glycine motif is arranged in parallel towards the binding pocket limiting wall. This yields an increased capability to incorporate space-demanding substrates.

Scheme 1, Henke et al.



Scheme 2a, Henke et al.



Scheme 2b, Henke et al.

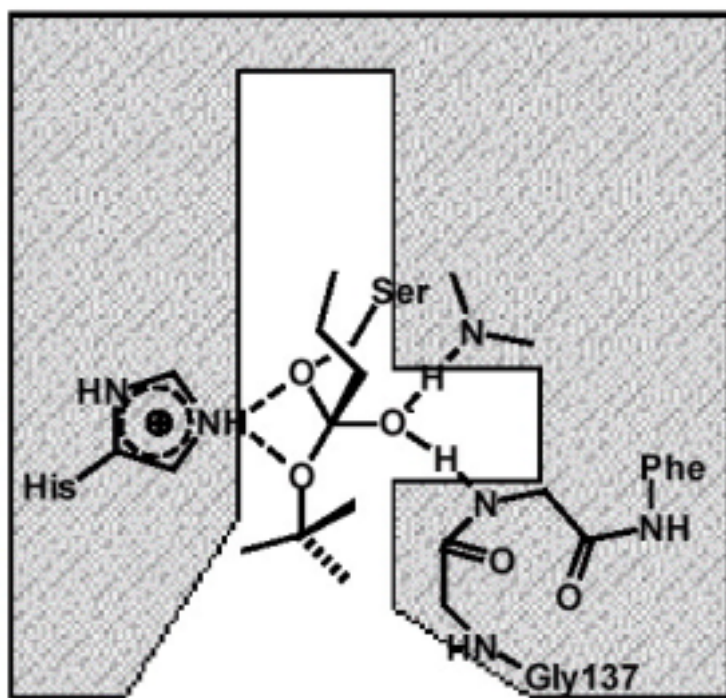


Table 1. Comparison of the distances between the proton at the active-site histidine's  $N_\epsilon$  and the carbonyl oxygen at the indicated oxyanion hole residue ( $N_{\epsilon, \text{HisH}} - O_{\text{Carb.}}$ ) for various GX- and GGX-type  $\alpha/\beta$  hydrolases.

Hydrolase	PDB entry	Type	Oxyanion hole residues	$N_{\epsilon, \text{HisH}} -$ $O_{\text{Carb.}}$ [ Å]
PCL	4LIP	GX	G <b>L17</b>	5.88
PAL	1EX9	GX	G <b>M15</b>	6.00
CVL	1CVL	GX	G <b>L17</b>	4.06
CAL-B	1TCA	GX	G <b>T65</b>	6.29
HLL	1TIB	GX	G <b>S83</b>	6.44
CRL	1LPM	GGGX	FGG <b>G134</b> F	7.76
BsubpNBE	Homology model	GGAX	FGG <b>A107</b> F	7.67
hAChE	1CLJ	GGGX	YGG <b>G122</b> F	7.48
eeAChE	1C2B	GGGX	YGG <b>G121</b> F	7.83
BACChE	Homology model	GGGX	YGG <b>G123</b> F	7.25

Table 2. Activity of hydrolases towards *t*-butyl acetate (**1**) compared to natural substrates: Activity was determined by pH-stat assay at pH 7.5 and 40°C (eeAChE: 25°C).

Hydrolase	Spec. activity	Spec.
	(natural substrate)	activity
	[ mU/mg Protein]	towards <b>1</b>
		[ mU/mg Protein]
CRL (Amano AYS)	44000 <sup>[ a]</sup>	10
GCL-B	83000 <sup>[ a]</sup>	no activity
EeAChE	200000 <sup>[ b]</sup>	no activity
CAL-A (Chirazyme L5, lyo)	117000 <sup>[ c]</sup>	50
PLE (Chirazyme E1, lyo)	157000 <sup>[ d]</sup>	80
(Chirazyme E2, lyo)	103000 <sup>[ d]</sup>	160
BsubpNBE	170000 <sup>[ c]</sup>	230

<sup>[ a]</sup> triolein; <sup>[ b]</sup> acetylthiocholine; <sup>[ c]</sup> tributyrin; <sup>[ d]</sup> ethyl butyrate

Table 3. Activity of GGGX-type hydrolases towards substrate **2-4**. Reactions very carried out at pH 7.5, 40°C (AChEs 25°C).

Enzyme <sup>[a]</sup>	<b>2</b>		<b>3</b>		<b>4</b>	
	<b>Time</b>	<b>Conversion</b>	<b>Time</b>	<b>Conversion</b>	<b>Time</b>	<b>Conversion</b>
	[ h]	[ %]	[ h]	[ %]	[ h]	[ %]
<b>PLE</b> , Chirazyme E-1, 390 U	2	53	8	48	0.5	50
<b>PLE</b> , Chirazyme E-2, 270 U	2	69	8	72	n.d. <sup>[ b]</sup>	n.d. <sup>[ b]</sup>
<b>CRL-CLEC</b> , 10 mg	2	56	8	23	0.5	77
<b>hAChE</b> , 37.5 U	24	17	48	5	4	39
<b>eeAChE</b> , 100 U	24	26	48	10	4	50
<b>bAChE</b> , 100 U	8	57	48	6	4	66
<b>CAL-A</b> , 480 U	24	41	48	71	2	59
<b>rec. BsubpNBE</b> , 350 U <sup>[ c]</sup>	0.8	50	0.6	50	0.3	50

<sup>[ a]</sup> Units refer to the activity towards the natural substrates given in Table 2, <sup>[ b]</sup> not determined

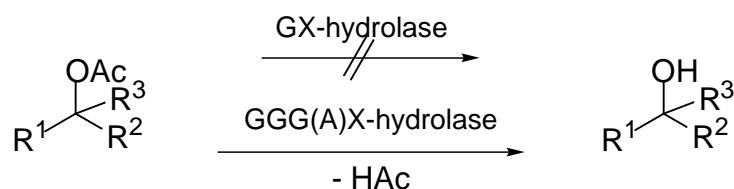


## Table of Contents

### A single amino acid pattern (GGG(A)X-motif) in hydrolases

controls their activity towards tertiary alcohols.

Consequently, a range of active lipases and esterases was identified by sequence comparison, which catalyze the efficient conversion of acetates of different tertiary alcohols rising access to this class of building blocks for organic synthesis, flavors and fragrances. Hydrolases bearing an alternative GX-motif were found inactive.



**Keywords:** biotransformations, enzyme catalysis, esterase, lipase, molecular modeling, tertiary alcohols

**Supplementary material** for the article "Activity of lipases and esterases towards tertiary alcohols: New insights into structure-function relationships" authored by E. Henke, J. Pleiss, U.T. Bornscheuer, submitted for the journal *Angewandte Chemie* (Z18885)

## **Experimental**

**Enzymes.** The following commercially available enzymes were donated by the named suppliers. From Amano (Nagoya, Japan): Amano AYS (Lipase from *Candida rugosa*), Lipase A Amano 6 (*Aspergillus niger* lipase (ANL)), Lipase AK Amano 20 (*Pseudomonas fluorescens* lipase (PFL)), Lipase D (*Rhizopus oryzae* lipase (ROL)), Lipase G Amano 50 (*Penicillium camembertii* lipase (PcamL)), Papain W40 (*Carica papaya*), Acylase (*Aspergillus* sp.); from Roche (Penzberg, Germany): Chirazyme L1-L12 (*Pseudomonas cepacia* lipase (PCL), *Candida antarctica* lipase B (CAL-B), *Candida antarctica* lipase A (CAL-A), *Pseudomonas* sp. lipase, Pig pancreatic lipase (PPL), *Thermomyces* sp. lipase, *Mucor miehei* lipase (MML), *Alcaligenes* sp. lipase). These enzyme preparations were used as delivered. Protein content was determined using the BCA Kit (Pierce, Rockford, IL, USA). Enzyme activity was determined by the pH-Stat assay as described below.

## **Cloning of the p-nitrobenzyl esterase from *Bacillus subtilis*.**

Genomic DNA from *Bacillus subtilis* DSM 402 was isolated using a standard protocol.<sup>[16]</sup> BsubpNBE was cloned by amplification of

the corresponding open reading frame from the genomic DNA using the primers EHE-pNBE-V2 (5'- ACT ACT ACT ACT CAT ATG ACT CAT CAA ATA GTA ACG -3') EHE-pNBE-R1 (5'- CTA CTA CTA CTA GGA TCC TTC TCC TTT TGA AGG-3'). The PCR product was digested by *Bam*HI and *Nde*I and ligated into an expression vector, based on pUC 19 under control of the strong regulating rhaP promotor (16), yielding plasmid pG-BsubpNBE.WT. This cloned BsubpNBE from DSM 402 differs in 11 residues from the BsubpNBE of strain NRRL B8079 as described by Zock et al.<sup>[17]</sup>

**Protein expression system.** Esterases from *Pseudomonas fluorescens*<sup>[10]</sup>, *Bacillus stearothermophilus*<sup>[11]</sup> and the p-nitrobenzyl esterase from *Bacillus subtilis* were expressed in *E. coli* using the corresponding plasmids (pG-PFEI.WT, pG-BsteE.WT and pG-BsubpNBE.WT) under control of a rhamnose inducible promoter, *rhaP*<sup>[14]</sup>, an ampicillin resistance served as selection marker. Esterase production was performed as described previously.<sup>[18]</sup> Recombinant AChEs were produced by expression in *Pichia pastoris* and the enzymes were kindly provided as crude extracts by S. Vorlova (Institute for Technical Biochemistry, Stuttgart University). Lipase B from *Geotrichum candidum* was expressed in *Pichia pastoris* as described by Catoni et al.<sup>[7]</sup>

**Directed evolution.** Random mutagenesis was performed by error-prone PCR<sup>[12]</sup> and DNA shuffling.<sup>[13]</sup> Mutated esterase encoding genes were ligated into the expression vector and transformed into *E. coli* DH5 $\alpha$ . Colonies were transferred into 384 well microtiterplates using a picking robot (Biorobotics,

Cambridge, UK) and grown in LB-Amp media supplemented with 5 % (v/v) DMSO. These plates were used as stocks enabling direct storage at - 80°C. Expression of esterase variants was performed by replica plating in 96 well microtiterplates containing LB-amp-rhamnose broth followed by incubation at 37°C for 20 h. Cell were disrupted by two freeze / thawing cycles. After centrifugation (4000 rpm, 10 min, 4°C), the cell lysate was used directly for activity testing towards TAEs using a pH-assay (see below). In addition, activity was determined spectrophotometrically using *p*-nitrophenyl acetate as described previously.<sup>[10c]</sup>

**pH-Assay.** The assay was performed in 96 well microtiterplates. To a substrate emulsion (180 µl / well containing 6 mM substrate, 10 % DMSO, 2 % gum arabic in sodium phosphate buffer 2 mM, pH 7.5) 6-carboxyfluorescein (10 µM) was added. Then cell lysate (20 µl / well) containing the recombinant esterase was added and fluorescence (ex.: 485 nm, em.: 538 nm, determined using the FLUOstar Galaxy fluorimeter from BMG Labtechnologies GmbH (Offenburg, Germany)) was measured immediately and after 20 h of incubation at 37°C.

**Synthesis of tertiary alcohol acetates.** Linalyl acetate (**2**) and *tert.*-butyl acetate (**1**) were purchased from Fluka (Buchs, Switzerland). All other acetates were prepared as follows.

**(*R,S*)-3-Methyl-1-pentin-3-yl acetate (**3**):** To 17 ml (*R,S*)-3-methyl-1-pentin-3-ol (19.6 g, 200 mmol) 20 ml acetic anhydride (15.7g, 154 mmol) was added dropwise while the flask was cooled with an ice bath. After adding 50 mg phosphorus

pentoxide and stirring for another 15 min the ice bath was removed and the mixture was stirred at room temperature for 16 h. The solution was washed twice with 100 ml water and extracted two times with 100 ml diethyl ether. The organic layers were combined and washed with saturated NaHCO<sub>3</sub> solution until no further formation of CO<sub>2</sub> was observed. The solution was washed again twice with water and dried with anhydrous Na<sub>2</sub>SO<sub>4</sub> before the solvent was removed in vacuum. The product was purified by flash chromatography on silica gel (petrol ether:ethyl acetate, 4:1) yielding the product as a colorless liquid (19.2 g, 68 % yield).

<sup>1</sup>H-NMR (500,15 MHz;  $\delta$  in ppm vs. TMS; in CDCl<sub>3</sub>)  $\delta$ : 1.03 (3 H; t; J = 7.5); 1.66 (3 H; s); 1.85 (1 H; m); 1.96 (1H; m); 2.03 (3 H; s); 2.55 (1 H; s). <sup>13</sup>C-NMR (125.76 MHz;  $\delta$  in ppm vs. TMS; in CDCl<sub>3</sub>)  $\delta$ : 8.40; 21.89; 25.90; 34.67; 73.18; 75.31; 83.75; 169.42.

**(*R,S*)-2-Phenyl-3-butin-2-yl acetate (4):** 25 g (*R,S*)-2-phenyl-3-butin-2-ol (171 mmol) was dissolved in 300 ml freshly distilled dry tetrahydrofuran. The solution was cooled on ice and 80 ml of 2.5 M butyllithium (200 mmol) in toluene was added dropwise over a period of 10 min. The mixture was stirred for 15 min before 15 ml freshly distilled acetyl chloride (211 mmol) was added. After removal of the ice bath, the mixture was heated under reflux for 1 h and then cooled to room temperature. Non-reacted acetyl chloride was hydrolysed by addition of 150 ml water. The mixture was extracted three times with 300 ml diethyl ether, the collected organic phases

were dried with anhydrous  $\text{Na}_2\text{SO}_4$  and solvent was removed in vacuum. Distillation (114°C, 15 mbar) yielded the product as a colorless liquid (24.5 g, 76 % yield).

$^1\text{H}$ -NMR (500.15 MHz;  $\delta$  in ppm vs. TMS; in  $\text{CDCl}_3$ )  $\delta$ : 1.89 (3 H; s); 2.07 (3 H; s); 2.80 (1 H; s); 7.34 (1H); 7.36 (2 H); 7.58 (2H).  $^{13}\text{C}$ -NMR (125.76 MHz;  $\delta$  in ppm vs. TMS; in  $\text{CDCl}_3$ )  $\delta$ : 21.71; 32.05; 75.31; 75.56; 124.75; 124.84; 127.91; 128.33; 128.38; 142.10; 168.62.

**Biotransformation.** Biotransformations were performed in a pH-Stat device (Metrohm, Switzerland) at 40°C. 20 ml of a preheated substrate emulsion (10 mM, stabilized with 2 % (w/v) gum arabic) were placed in the reaction chamber and the enzyme preparation was added. The pH-value was kept constant by automatic addition of NaOH solution. Esterase activity and conversion were calculated from NaOH consumption. In addition, samples (200  $\mu\text{l}$ ) were withdrawn from the reaction mixture and extracted with isohexane (1 ml). Enantiomeric excess of substrate and product were determined by gas chromatography.

**Gas chromatography.** Determination of optical purity was performed using gas chromatography on a chiral column (Heptakis-(6-*O*-pentyl-2,3-di-*O*-methyl)- $\gamma$ -cyclodextrin in OV1701, 25 m; Prof. König, Hamburg University, Hamburg, Germany) with hydrogen (40 kPa) as carrier. Conditions: linalyl acetate/linalool: 90°C, 25 min; (*R,S*)-3-methyl-1-pentin-3-yl acetate/(*R,S*)-3-methyl-1-pentin-3-ol: 40°C, 0 min-2°C/min-55°C, 10 min; (*R,S*)-2-Phenyl-3-butin-2-yl acetate/(*R,S*)-2-phenyl-3-butin-2-ol: 120 °C, 15 min.

## **Molecular modeling.**

**Software, force field:** Molecular modeling was performed using a Silicon Graphics Octane 2 workstation (SGI, Mountain View, CA) and the Sybyl 6.1 (Tripos, St. Louis, MO) software. For all calculations, the Tripos force field was utilized. Gasteiger-Hückel charges were used, the charges of the catalytic His<sub>act.</sub> and the tetrahedral Ser<sub>act.</sub>-substrate complex were adjusted as described by Holzwarth *et al.*<sup>[19]</sup>

## **Structures, homology modeling, substrate docking.**

Experimentally determined X-ray structures of CRL (PDB entry 1LPM) and eeAChE (PDB entry 1C2B) from a homology model of hAChE (PDB entry 2CLJ) were used. A homology model of BsubpNBE DSM 402 was created using the X-ray structures of the corresponding enzyme from strain NRRL B8079 (PDB entries 1QE3, 1C7J, 1C7I).<sup>[20]</sup> The homology model for bAChE was based on the structure of AChE from *Torpedo californica* (PDB entry 1QIK, 1CFJ). The homology models were computed using the Swiss-Model automated modeling service of GlaxoSmithKline (<http://www.expasy.ch/swissmod/SWISS-MODEL.html>).

All possible solvent molecules included in the PDB files were removed before substrate docking. Substrates were manually docked into the binding site of the enzymes, mimicking the tetrahedral intermediate formed after the nucleophilic attack of the catalytic Ser<sub>act.</sub>. This resembles the rate-limiting step of ester hydrolysis. The substrate was orientated with the oxyanion towards the oxyanion hole

residues and the protonated N<sub>ε</sub> of His<sub>act</sub> embedded between the O<sub>γ</sub> and the O<sub>ester</sub> of the substrate. The substrates' substituents were orientated in the binding pocket to a minimum of repulsive interaction with the protein structure.

**Minimization, molecular dynamics simulations.** The enzyme-substrate complex was refined first by minimization. Next, a molecular dynamics simulation was performed for 18 ps (2 ps at 5K, 2 ps at 30 K, 2 ps at 70 K; 12 ps at 100 K). The coupling constant was adjusted to 10 fs. The non-bonded interaction cut-off was set to 8 Å, the dielectric constant to 1.0. The conformers were saved every 40 fs. An average structure over the last 2 ps was calculated and used for analysis. All minimization and MD simulations were performed *in vacuo*, with constrained protein backbone.

To ensure that the results do not depend on the choice of the initial conformation, additional simulations of the same enzyme-substrate complex were performed using different initial conformations. Also, it was verified that a simulation time of 18 ps is sufficient extending the simulations to 100 ps. This prolonged simulation time led to same results as the 18 ps runs.